BMC Neuroscience

RESEARCH

Open Access

Structural-functional connectivity decoupling in multiscale brain networks in Parkinson's disease

Ting Zou[1,2†], Chen Chen[3†], Huafu Chen[1,2*], Xuyang Wang[1,2], Lin Gan[1,2], Chong Wang[1,2], Qing Gao[4], Chunyan Zhang[3], Wei Liao[1,2], Jingliang Cheng[3*] and Rong Li[1,2*]

Abstract

Background Parkinson's disease (PD) is a progressive neurodegenerative disease associated with functional and structural alterations beyond the nigrostriatal dopamine projection. However, the structural-functional (SC-FC) coupling changes in combination with subcortical regions at the network level are rarely investigated in PD.

Methods SC-FC coupling networks were systematically constructed using the structural connectivity obtained by diffusion tensor imaging and the functional connectivity obtained by resting-state functional magnetic resonance imaging in 53 PD and 72 age- and sex-matched healthy controls (HCs). Then, we explored how SC-FC coupling varied within and between several well-defined functional domains.

Results Results showed that the SC-FC coupling in patients with PD was globally reduced in comparison with HCs. Specifically, regional SC-FC decoupled in the inferior parietal lobule, occipitotemporal cortex, motor cortex, and higher-order association cortex in patients with PD. Moreover, PD showed intranetwork SC-FC decoupling in the visual network (VIS), limbic and higher-order association networks. Furthermore, internetwork decoupling mainly linked to the VIS, the somatomotor network (SOM), the dorsal attention network, and the default mode network, was observed, increased internetwork coupling was found between the subcortical network and the SOM in PD (all $p < 0.05$, FDR corrected).

Conclusions These findings suggest that PD is characterized by SC-FC decoupling in topological organization of multiscale brain networks, providing insights into the brain network mechanisms in PD.

Keywords Parkinson's disease, Multiscale brain networks, Structural-functional coupling

†Ting Zou and Chen Chen contributed equally to this work.

*Correspondence:
Huafu Chen
chenhf@uestc.edu.cn
Jingliang Cheng
fccchengjl@zzu.edu.cn
Rong Li
rongli1120@gmail.com

[1]The Clinical Hospital of Chengdu Brain Science Institute, School of Life Science and Technology, University of Electronic Science and Technology of China, Chengdu 610054, P.R. China
[2]School of Life Science and Technology, MOE Key Laboratory for Neuroinformation, High-Field Magnetic Resonance Brain Imaging Key Laboratory of Sichuan Province, University of Electronic Science and Technology of China, Chengdu 610054, P.R. China
[3]Department of MRI, the First Affiliated Hospital of Zhengzhou University, Zhengzhou 450052, P.R. China
[4]School of Mathematical Sciences, University of Electronic Science and Technology of China, Chengdu 611731, P.R. China

Introduction

Parkinson's disease (PD) is a neurodegenerative disease predominantly characterized by motor impairments derived from the severe loss of dopaminergic neurons in the substantia nigra pars compacta [1]. Non-motor symptoms, such as anxiety, dementia, visual dysfunction, and depression, are considered to be part of the clinical spectrum of PD [2, 3]. The neuropathological substrate of such motor and non-motor manifestations involves multiple regions and neurotransmitter systems [4, 5]. Previous studies have shown widespread alterations in brain structural connectivity (SC) and functional connectivity (FC) among patients with PD, particularly in subcortical (SUB) striatum, motor cortex, and cortical higher-order association areas [6–8]. A neuroimaging study suggested that the SC network may be the physical substrate of the FC network and the combined modalities could enrich the understanding of these canonical brain networks [9]. Yet, the relationship between the FC and SC at a network scale in PD remains poorly understood.

Recent publications mapping connectome properties to clinical features have focused on using either FC or SC alone, or concatenating both together to reveal brain-behavior relationships. Neuroscientific investigations have shown alterations in the SC network in PD. For instance, impaired white matter and gray matter structural connections involving cortical and SUB regions, such as precentral gyrus, insula, hippocampus, subthalamic nucleus, substantia nigra, and striatum, were identified in PD [10, 11]. In addition to the abnormal structural network properties, patients with PD exhibited alterations in functional network parameters. In particular, study have shown that patients with PD exhibited decreased functional integration across neural networks such as striatum, mesolimbic cortex, and sensorimotor regions, and the prevalent disconnection in mesolimbic-striatal loops is associated with some early clinical non-motor features in PD [12]. Moreover, cognitive decline in PD was found to be associated with FC damage in brain regions, especially in the posterior parts [13, 14]. Our recent work revealed attenuated brain white-matter functional interactions in PD, and these abnormalities were associated with clinical motor and non-motor symptoms [15]. However, these studies mainly focused on single network property. Brain network dysfunction has been hypothesized to have resulted from abnormalities in anatomic connections and functional interactions of distributed brain regions [16]. Another study assumed a relationship between the strength of an SC between two brain areas and the strength of the corresponding FC [17]. In addition, SC places anatomical constraints on FC in the network [18]. In turn, FC has an effect on SC through brain plasticity [19, 20]. Therefore, mapping the functional and structural connectivity could expand the understanding of synchronization alterations in PD.

SC-FC coupling, as an integrated measurement linking a functional network with a structural network, is considered to be more sensitive than any single modal index in detecting subtle changes in brain activity [21]. Studies have shown that changes in SC-FC coupling occur not only during brain maturation [22] but also in neurological disease [21]. A recent paper showed that SC-FC decoupling in PD followed an unimodal-to-transmodal gradient, and SC-FC became more decoupled in regions higher along the unimodal-transmodal hierarchy [23]. However, since it is well known that subcortical structures play an important role in patients with PD [24, 25], and previous studies mainly focused on investigating the relationship between SC and FC in the cortical brain regions, while ignoring whether SC-FC coupling was altered in subcortical regions. Moreover, as the human brain is a complex network that is functionally segregated and integrated simultaneously via specific connectivity patterns [26], investigating the large-scale (whole brain) SC-FC coupling only may not be sufficient. Therefore, exploring SC-FC associations in combination with subcortical regions at the network level may provide deeper insights into the mechanism underlying PD.

In this study, how SC-FC coupling was altered in a multiscale network of 53 patients with PD and 72 age-matched healthy controls (HCs) was investigated using resting-state functional magnetic resonance imaging (fMRI) and diffusion tensor imaging (DTI). On the basis of the results of widespread topological disruption of SC and FC networks across the whole brain, SC-FC coupling was hypothesized to be affected at the whole-brain and multiscale network levels in PD. Therefore, whether regional SC-FC coupling showed any changes was first identified. Next, the specific pattern of abnormal SC-FC coupling in PD was analyzed at the network level.

Materials and methods

Study setting and participants

The data of all participants with PD and HCs were obtained in the First Affiliated Hospital of Zhengzhou University. A written informed consent was obtained from all subjects. A total of eighty-five right-handed patients with PD and eighty-three HCs were initially recruited. Patients with PD were diagnosed by at least two or more experienced neurologists in accordance with UK PD Society Brain Bank criteria [27]. Patients underwent neurological examinations that included a medical interview. Their motor status were evaluated using part III of the Unified Parkinson's Disease Rating Scale (UPDRS III) [28] and Hoehn-Yahr (H&Y) stage [29]. For H&Y stages, all patients with PD were diagnosed with mild to severe stages of the disease (stages 1–5); a high

score suggested advanced disease stage. Patients were assessed in an off-medication state (12 h after withdrawal of dopaminergic drugs). Exclusion criteria included incomplete data acquisition (e.g., incomplete MRI scanning and pivotal clinical scores), head motion > 3 mm and head rotation > 3°. Moreover, none of the patients had undergone deep brain stimulation or other brain surgery. Finally, fifty-three right-handed patients with PD (mean ± SD = 58.42 ± 8.47 years; 20 men) and 72 right-handed HCs (mean ± SD = 58.99 ± 10.02 years; 36 men) were included in the current study. The demographic characteristics of the study participants are provided in Table 1, and the participant-specific exclusion procedure is shown in Supplementary Fig. 1.

Imaging data acquisition

A 3T Siemens Prisma MR scanner in the Fist Affiliated Hospital of Zhengzhou University was used to collect MRI data. For acquisition of the fMRI data, the subjects were asked to close their eyes and remain at rest without thinking about anything or falling asleep. A high-resolution functional image was acquired using a multiband echo-planar imaging sequence (acceleration factor of 4) with the following parameters: voxel size = 2.0 mm × 2.0 mm × 2.64 mm; repetition time (TR) = 1000 ms, echo time (TE) = 30 ms, matrix size = 110 × 110, field of view (FOV) = 220 mm × 220 mm, flip angle = 70°, slice thickness = 2.2 mm, and 52 slices. For each subject, a total of 400 volumes were obtained from the scan time of 8 min. Structural images were also acquired using a magnetization-prepared rapid gradient-echo sequence with the following parameters for co-registration with functional images: TR = 2300 ms, TE = 2.9 ms, flip angle = 9°, slice thickness = 1.2 mm, slices = 176, FOV = 240 mm × 256 mm, matrix size = 240 × 256, and voxel size = 1 mm × 1 mm × 1.2 mm. Furthermore, DTI data were obtained with a single-shot EPI sequence by using the following parameters: 69 directions, TR = 9200 ms, TE = 54 ms, flip angle = 90°, slice thickness = 2 mm, FOV = 256 mm × 256 mm, matrix size = 128 × 128, and b = 1000 s/mm^2. These data were used for analysis after quality assurance.

Anatomical parcellation

Similar to [30, 31], the present study used a volume labelled with the Schaefer labels, plus the labels referring to Freesurfer's aseg parcellation of the subcortical areas. A total of 400 cortical regions of interest (ROIs) were generated by segmenting each participant's T1-weighted image. This template was defined by the similarity of global FC and local FC gradients and has been widely used in previous studies, revealing physical meaningful features of brain organization and superior functional and connectional homogeneity relative to other parcellations, which was widely used to estimate brain network [32]. In addition, 12 subcortical regions anatomically derived from FreeSurfer's aseg volume were used, including the bilateral hippocampus, caudate, thalamus, putamen, pallidum, and amygdala. For examination of the network-level effect of SC-FC coupling and evaluation of between-group differences, the canonical seven-network parcellation given by Yeo et al. [33] was used to define functional modules, and each node from the Schaefer-400 template was assigned to one of the seven networks: visual network (VIS), somatomotor network (SOM), dorsal attention network (DOR), ventral attention network (VEN), limbic network (LIM), and frontoparietal control network (FPC) and default mode network (DMN). The subcortical regions were considered as a single network, and eight networks were finally included in this study (Supplementary Table 1). The same parcellation was used to construct SC and FC matrices for each participant.

SC network construction

Most commonly, SC is inferred from diffusion tensor imaging, which offers the opportunity to reliably construct whole brain white matter networks from fiber tractography. Using DTI images, physical network

Table 1 Clinical and demographic characteristics of participants

Demographics	PD (*n* = 53)	HCs (*n* = 72)	PD vs. HCs
	Mean ± SD (Min-Max)	Mean ± SD (Min-Max)	*P*-value
Gender (male/female)	20/33	36/36	0.17[a]
Age (years)	58.42 ± 8.47 (41–73)	58.99 ± 10.02 (36–76)	0.71[b]
Duration (years)	3.23 ± 2.84 (0.25-10)	/	/
Hoehn-Yahr	2.03 ± 0.83 (1–5)	/	/
UPDRS III	23.70 ± 14.09 (7–74)	/	/
UPDRS	39.92 ± 18.15 (15–101)	/	/
MMSE	22.83 ± 3.92 (12–29)	/	/
Mean FD (mm)	0.10 ± 0.03 (0.052–0.196)	0.11 ± 0.04 (0.048–0.198)	0.1006[b]

Abbreviations: Values are presented as mean ± standard deviation. PD, Parkinson's disease; HCs, healthy controls; MMSE, Mini-mental State Examination; UPDRS, United Parkinson's Disease Rate Scale; FD, frame-wise displacement

[a] χ^2 test

[b] Nonparametric Mann-Whitney tests

connections, and both cortical and subcortical structures and their interconnectedness can be studied. Moreover, because of the intrinsic integration of white matter/gray matter and the complementary information embedded in DTI/fMRI techniques, combining DTI and fMRI data becomes an increasingly important methodology in clinical neuroscience fields [34]. In our study, DTI images were preprocessed in MRtrix 3.0 (https://www.mrtrix.org/). Diffusion-tensor images underwent denoising, removal of Gibbs artifacts, eddy-current and motion correction, and bias field correction. The diffusion tensor metric was calculated, and constrained spherical deconvolution was performed to estimate the white-matter fiber direction distribution function on the basis of the expected signal of a single-fiber white matter population (the so-called response function) [35]. Individual T1- weighted images were first co-registered to the b0 image in DTI native space by using antsRegistrationSyNQuick (ANTs version 2.1.0), and five-tissue anatomical segmentation was performed using the 5ttgen script in MRtrix. Similarly, the cortical and SUB atlases were then transformed to each participant's native space with nearest neighbor interpolation. For each participant, probabilistic (iFOD2) [36], anatomically constrained tractography (ACT) [37] algorithm with voxel-wise directional uncertainty fractional anisotropy (FA) > 0.2, direction change < 60° were used to create the individual, whole-brain tractograms containing 0.2 million streamlines. The SC between any two regions was the SIFT2-weighted [38] sum of streamlines connecting those regions divided by the sum of the gray-matter volume of those regions, resulting a symmetric 412×412 ROI-volume SC matrix for each subject. Then, we calculated the separate SC strengths at the regional and the network level, respectively. Regional SC strength was calculated as the mean of all connectional weights within the brain regions. Intranetwork connectivity strength is an evaluation index for the significance of a particular network within the brain networks, which is calculated as the mean of all connectional weights within the network. The internetwork connectivity strength between two networks is the mean of the connectional weights connecting both networks.

FC network construction

The functional images preprocessing were carried out using Statistical Parametric Mapping toolkits (SPM12, https://www.fil.ion.ucl.ac.uk/spm/software/spm12/) and Data Processing Assistant for Resting-State fMRI (DPARSF v5.0, http://www.restfmri.net) software. All analyses in this study were performed in MATLAB 9.5 environment (https://www.mathworks.com). First, all images were reoriented to adjust the image origins at the anterior commissure by manual setting after artifact checking and format conversion. Subsequently, the first 10 volumes were discarded to stabilize the time series, and the remaining 390 volumes were corrected for realignment. For each participant, the T1 images were co-registered to the functional images and segmented into gray matter, white matter, and cerebrospinal using DARTEL [39]. In addition, in the native functional image space, spurious signals derived from linear and quadratic trends, Friston-24 head motion parameters, white matter, and cerebrospinal tissues were regressed out using CompCor method (i.e., five principle components of noisy signals) [40]. Then, the images were warped into the standard Montreal Neurological Institute space and resampled to 2 mm × 2 mm × 2 mm voxel resolution. Finally, the residual images were spatially smoothed with a 4 mm full-width half-maximum isotropic Gaussian kernel and temporal bandpass filter (0.01-0.1 Hz) was used to reduce the effects of low-frequency drift and high-frequency noise [41]. The excluded criteria of head motion were head translation > 3 mm, head rotation > 3°, and mean frame wise displacement (FD) > 0.2 mm. FC between ROIs was quantified as the Pearson correlation coefficient between mean regional BOLD time series, and followed by application of Fisher transform. Subsequently, the separate FC strengths at the regional and the network level were calculated in accordance with the aforementioned SC calculation method.

Regional -level SC-FC coupling

The strength to which a brain region's SC relates to coordinated fluctuations in neural activity between regions was quantified to characterize how SC-FC coupling changes in PD. For each subject, SC-FC coupling was performed to assess the correlation between the strength of the SC and that of the FC. Specifically, to minimise the effect of spurious connections whilst avoiding arbitrary thresholds, the non-zero SC network and the corresponding FC edges for each region were extracted to represent as vectors of connectivity strength from a single node to all other nodes. As the previous study [22, 23], the negative FC was preserved unless the anatomical connection did not survived. We chose non-parametric Spearman-rank correlation to quantify the similarity of a region's structural and FC pattern to the rest of the brain as it is a measure that is straightforward and easily interpreted, importantly, accommodates the non-Gaussianity of the entries in the SC. Therefore, a vector of length of 412 that represents the regional SC-FC coupling strength for each individual was generated.

Network-level SC-FC coupling

The between and within-network couplings were separately calculated to identify whether the relationship between the strength of the SC and that of the FC

varied widely across brain networks. For each region, the within-network SC-FC coupling denoted the Spearman correlation of the SC and FC between that region and other regions in the same network. The group-averaged network was computed by averaging the SC-FC coupling in each network. Differently, the between-network SC-FC coupling was calculated as follows: first, the upper triangle of the SC and FC matrices associated with each two networks were extracted for each individual subject. Subsequently, these non-zero values of SC and the corresponding FC were correlated across subjects within the HCs and PD groups separately. On the basis of the above analysis, a two-sample *t*-test was applied to compare the corresponding SC-FC coupling strength among 28 pairs of network in the HCs and PD groups. An overview of the study methodology is shown in Fig. 1.

Complementary analyses

There has been increased interest in identifying subtypes of PD and understanding the heterogeneity in clinical symptoms [42]. Substantial heterogeneity between individual patients in the clinical presentation of PD has led to the classification of distinct PD subtypes. Therefore, as a preliminary study, we subdivided all PD patients into several clinical categories for further study. For cognitive subtypes, PD patients were categorized into two subgroups according to MMSE scores [43] (subgroup 1: 26-30, $n=14$; subgroup 2: 0-26, $n=39$). For motor subtypes, all patients were categorized into two subgroups based on H&Y scales [11] (subgroup 1: 1–2, $n=32$; subgroup 2: 2.5–5, $n=21$). In addition, we also performed several ancillary analyses to verify the robustness of our SC-FC coupling results in terms of covariance regression, atlas definition and head motion scrubbing. First, to investigate whether the brain SC-FC coupling was potentially influenced by age and sex, we reanalyzed the case-control differences with age and sex as covariates. Second, to validate the main findings with the functionally defined 412 atlas, we also used an anatomically derived 212 region atlas, with 200 cortical regions from Schaefer-200 and 12 subcortical regions from FreeSurfer's aseg volume. Third, we also included the scrubbing procedure during the fMRI data preprocessing to reduce the potential confounding influence of head motion on the main results. During the scrubbing process, we used the "cut" option available in the DPABI toolbox with a threshold for "bad" time points of 0.5 (one time point before and two "bad" time points after) [44].

Statistic analysis

For the practical significance, the effect size of network deviations was calculated as the Cohen's *d* value between the PD and HCs. For the statistical significance, significant SC-FC coupling changes were examined by the two-sample *t*-test or nonparametric Mann-Whitney tests, depending on whether the data were normally distributed [45]. Statistical tests were False discovery rate (FDR) corrected to reduce the type I errors. In addition, to further investigate the relationship between brain features and clinical performances, we performed correlation analysis between the regions with significant altered SC-FC coupling and other variables (H&Y, UPDRS, disease duration and MMSE score).

Results

Regional SC-FC decoupling in PD

Under the constraint of non-zero structural connections, correlation analysis was performed between FCs and their structural counterparts in the whole-brain network across participants. The group average SC-FC coupling over 412 ROIs is shown in Fig. 2A. The regional SC-FC coupling was almost entirely positive, ranging from 0 to 0.42 in HCs and from 0 to 0.39 in patients with PD in the present study. In both groups, SC-FC coupling varied greatly across cortical and SUB areas, with higher coupling in primary sensory and medial prefrontal cortex and lower coupling in lateral temporal, frontoparietal, and SUB regions. Compared with HCs, 14 nodes of all 412 nodes across the whole brain showed significant reduced coupling in PD (Fig. 2B, $p<0.05$, FDR corrected). Decreased regional SC-FC coupling was found in the bilateral middle temporal areas and inferior parietal lobe, left middle occipital gyrus, postcentral gyrus and superior temporal areas, right cuneus and precuneus gyrus, supramarginal gyrus, angular gyrus, anterior and middle cingulate cortex, and insula. The most deceased SC-FC coupling was observed in the right inferior parietal lobe of patients with PD. The correlation was observed between the SC-FC coupling strength in this region and disease duration (r = -0.2911, $p=0.0344$). At the whole-brain level, the average SC-FC coupling across the whole-brain network was compared between HCs and PD group, the results showed that patients with PD displayed significant reduced global coupling compared with HCs (t = -4.178, $p<0.001$, Fig. 2C).

Decreased intranetwork SC-FC coupling in PD

The mean intranetwork SC-FC coupling strength of each region is presented in Fig. 3. The network level analysis revealed that the SC-FC coupling varied widely within each network in the PD and HCs. Compared with the HCs , the PD group showed significant decreased SC-FC coupling in VIS, DOR, LIM, and FPC and DMN (Fig. 3, Supplementary Table 2, $p<0.05$, FDR corrected).

Altered internetwork SC-FC Coupling in PD

How coupling was altered between specialized networks was further identified. Compared with HCs, altered

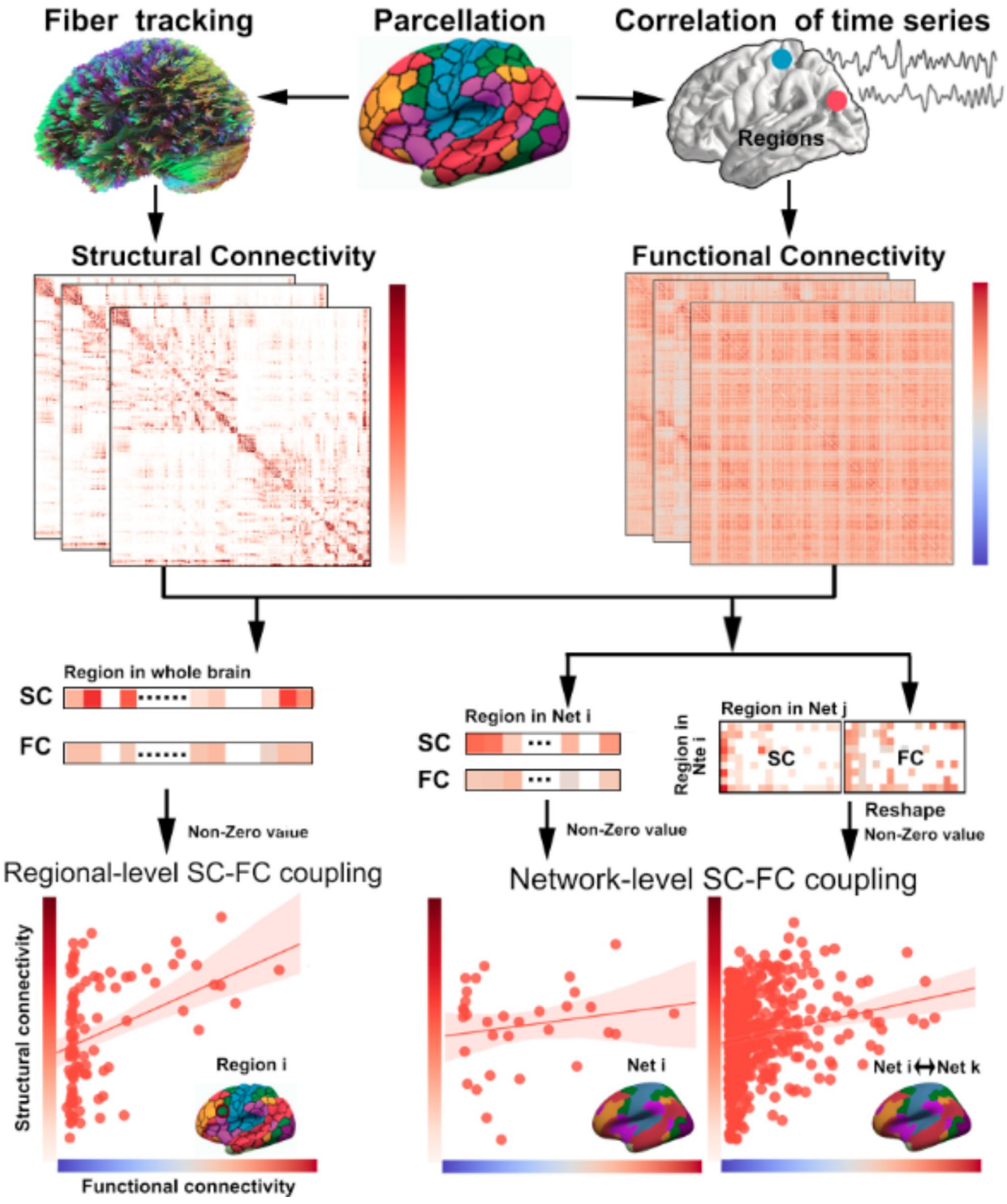

Fig. 1 Workflow for quantifying regional SC-FC coupling. Schaefer-400 cortical parcellation and 12 subcortical regions (hippocampus, caudate, thalamus, putamen, pallidum, and amygdala from FreeSurfer's aseg volume for each hemisphere) were included, resulting in 412 network nodes. For each participant, the regional SC-FC coupling was the Spearman-rank correlation between a region's non-zero SC and the corresponding FC. The intranetwork SC-FC coupling for each region was the Spearman rank correlation between the non-zero elements of regional SC and FC profiles in the same network. Internetwork SC-FC coupling was calculated by first extracting all connections between each two networks for SC and FC. Subsequently, these non-zero values for SC and FC were correlated across subjects within the HCs and PD groups separately. SC, structural connectivity; FC, functional connectivity

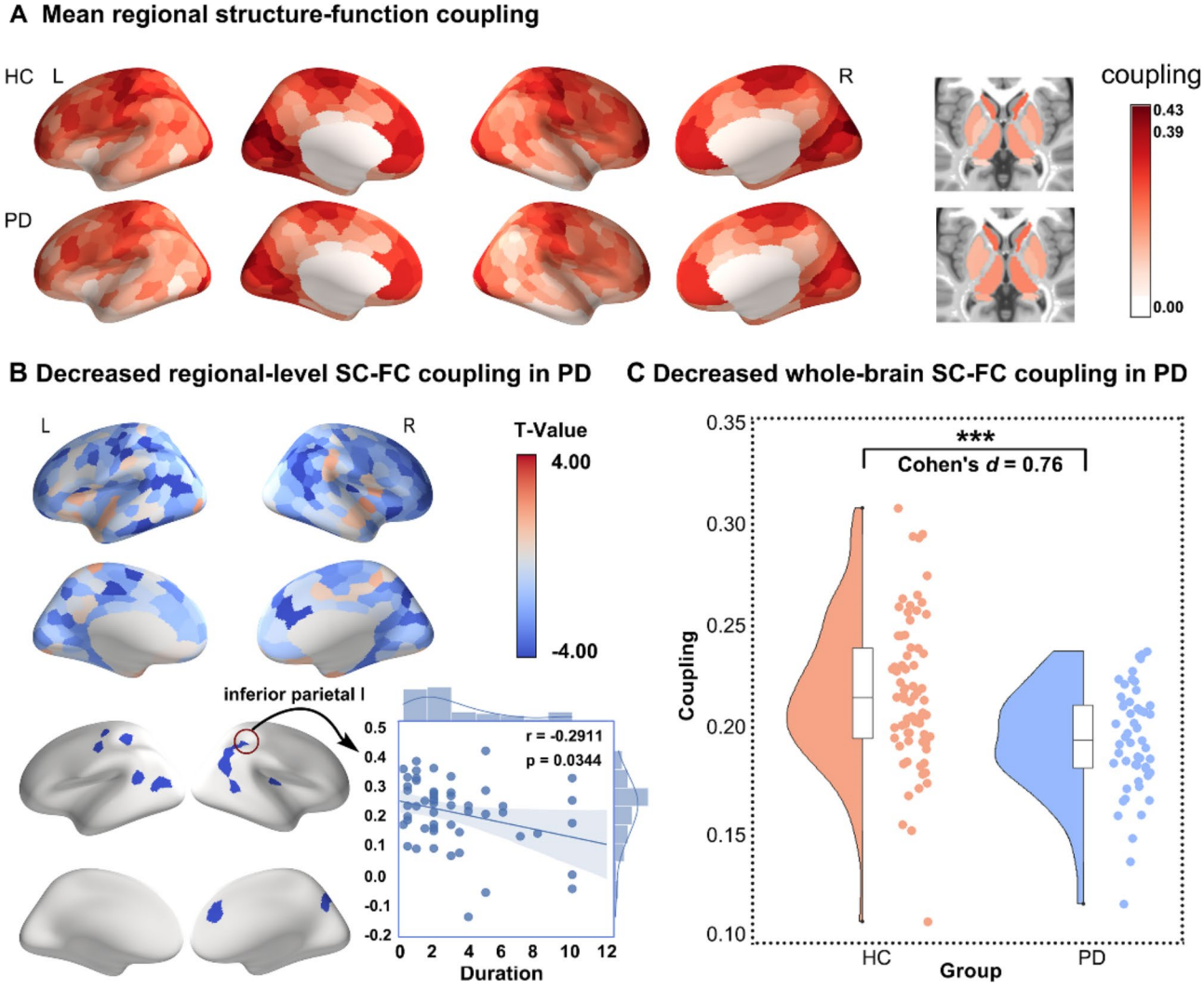

Fig. 2 SC-FC coupling changes in patients with PD. (**A**) Spatial pattern of SC-FC coupling in HCs and PD. The coupling between regional SC and FC profiles varied widely across the cortex, similar in both groups. Primary sensory and medial prefrontal cortex exhibited relatively high SC-FC coupling, while lateral temporal and parietal regions showed relatively low coupling. (**B**) Spatial pattern of SC-FC decoupling for each node across the brain in PD. Decreased regional SC-FC decoupling was found in the bilateral middle temporal areas and inferior parietal lobe, left middle occipital gyrus, postcentral gyrus and superior temporal areas, right cuneus and precuneus gyrus, supramarginal gyrus, angular gyrus, anterior and middle cingulate cortex, and insula ($p < 0.05$, FDR corrected). The strength of SC-FC coupling in the right parietal lobe was negatively correlated with disease duration in patients with PD ($r = -0.2911$, $p = 0.0344$, uncorrected). (**C**) Average SC-FC coupling changes across all nodes in PD. Data were analyzed by using two-sample *t*-tests. *** denotes statistically significant results ($p < 0.001$). SC, structural connectivity; FC, functional connectivity; HCs, healthy controls; PD, parkinson's disease; L, left; R, right

internetwork SC-FC coupling strength was found in 9 of 28 pairs of networks (Fig. 4 and Supplementary Table 3, $p<0.05$, FDR corrected). Specifically, statistical analysis identified significant decreased coupling strength between SUB and VIS; SOM and DOR, VEN; DOR and DMN, FPC, LIM; DMN and FPC and LIM. Meanwhile, increased internetwork coupling was found between SUB and SOM in patients with PD. The SC-FC coupling strength between DOR and DMN was correlated with UPDRS III scores ($r = -0.276$, $p=0.0455$).

Complementary results

At the regional level, no significant SC and FC difference between the HCs and PD group was found. At the network level, patients with PD showed increased intranetwork FC strength within the DMN (t = -3.08, $p=0.0026$, FDR corrected) and preserved SC strength in all networks (Supplementary Fig. 2). In contrast, no significant difference in the internetwork SC and FC strength was found between the groups. For subtype analysis, compared with HCs, MMSE score-specific subgroup comparisons revealed decreased SC-FC coupling in subgroup 1 (t = -3.07, $p=0.0028$) and subgroup 2 (t = -3.36, $p=0.0011$),

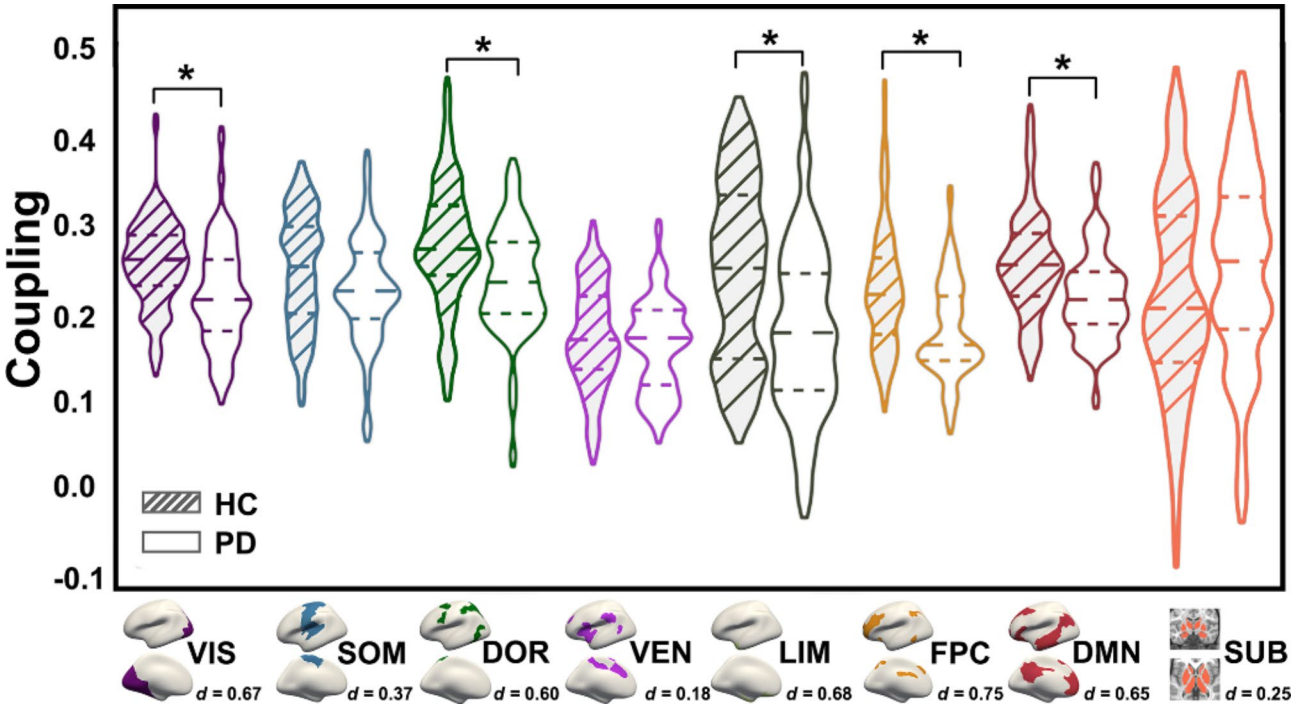

Fig. 3 Intranetwork SC-FC decoupling in PD. Patients with PD had significant decreased SC-FC coupling in the VIS, DOR, LIM, and FPC module and DMN. Absolute cohen's *d* value is shown around the distribution. VIS, visual network; SOM, somatomotor network; DOR, dorsal attention network; VEN, ventral attention network; LIM, limbic network; FPC, frontoparietal control network; DMN, default mode network; SUB, subcortical network. * denotes statistically significant results ($p < 0.05$, FDR corrected)

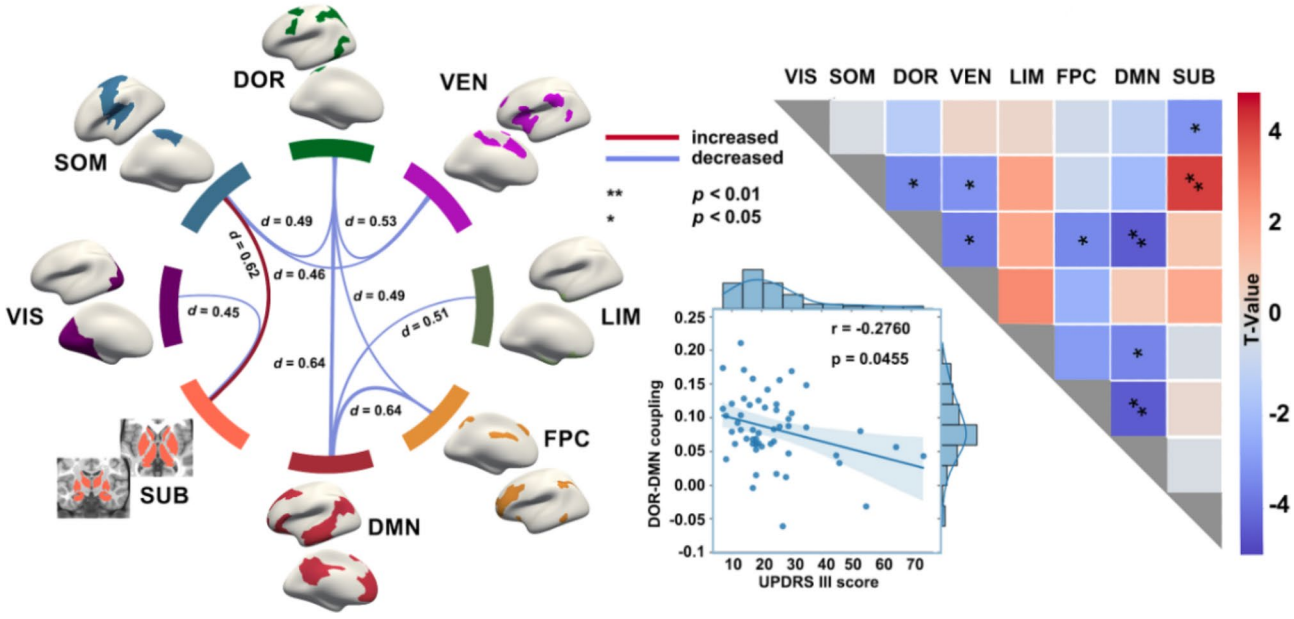

Fig. 4 Internetwork SC-FC coupling changes in PD. Statistical analysis revealed altered internetwork SC-FC coupling strength in 9 pairs of modules. Specifically, the coupling strength between SUB and VIS networks; SOM and DOR, VEN; DOR and DMN, FPC, VEN networks; DMN and FPC and LIM networks decreased in PD, while increased internetwork coupling was found between the SUB and SOM network. The coupling strength between DOR and DMN was correlated with UPDRS III scores ($r = -0.276$, $p = 0.0455$, uncorrected). Edges with warm and cool colors in the wheel represent increased and decreased coupling values. The size of the edges reflects the t values for coupling associated with significant alteration in PD. Cohen's *d* value is shown around the distribution. VIS, visual network; SOM, somatomotor network; DOR, dorsal attention network; VEN, ventral attention network; LIM, limbic network; FPC, frontoparietal control network; DMN, default mode network; SUB, subcortical network. * denotes statistically significant results ($p < 0.05$, FDR corrected)

and H&Y score-specific subgroup comparisons showed decreased SC-FC coupling in subgroup 1 (t = -2.98, p=0.0038) and subgroup 2 (t = -3.44, p=<0.001). No significant difference was found between PD subgroups (Supplementary Fig. 3). In addition, when gender and age were considered as covariates, results revealed a similar brain SC-FC decoupling patterns in patients with PD (Supplementary Figs. 4–6). We also see good agreement with the main SC-FC decoupling when using 212 region atlas (Supplementary Figs. 7–9) and FC preprocessed with motion scrubbing (Supplementary Figs. 10–12).

Discussion

In this study, the SC-FC relations at the nodal, intra-, and inter-network levels were systemically investigated in patients with PD. Compared with the HCs, the patients with PD exhibited a spatially widespread decoupling of SC-FC correlations, suggesting broken macroscopic network organization across the brains of these patients. Importantly, at the network level, significantly decreased SC-FC coupling was found in the VIS, DOR, LIM, and FPC modules and DMN among patients with PD. Furthermore, these patients demonstrated decreased internetwork coupling mainly linked several modules, including VIS, SOM, DOR, and DMN, while increased internetwork coupling was observed between the SUB and SOM modules. The reduced whole-brain coupling and discrepant SC-FC coupling changes at the network level reflected disturbed segregation and integration of complex networks in patients with PD, thus providing avenues to further understand the pathophysiological network mechanisms underlying PD.

Changes in brain structure and function have been extensively investigated with neuroimaging studies in order to reveal the pathophysiology of PD. Consistent with the findings of previous studies that aimed to characterize the structural and functional network correlation in large-scale brain networks [22, 40], participants showed a clear positive correlation between the whole-brain functional and structural network correlation matrices. Compared to a recent study that examined how the relationship between structural and FC changes in PD [23], our study revealed a similar SC-FC decoupling pattern in cortical regions, particularly in the inferior parietal lobule, occipitotemporal cortex, motor cortex, and higher-order association cortex with and without thresholding. Studies of fiber tracking based on DTI showed that there was structural connection of white matter fiber among the nodes of resting-state functional network, illuminating that gray matter region of functional network was based on connection of white matter networks [46]. Reduced SC constraints on FC may be a possible fundamental mechanism that explains the perception-motor processing deficits in PD patients. The higher prevalence of neurocognitive deficits observed in PD, such as hallucinations and delusions, may be attributed to decoupling in higher-order regions. The right inferior parietal lobules were active, and they played an important role during various visuospatial tasks [47]. The negative correlation between the coupling strengths in the inferior parietal lobule and durations further indicated that SC-FC decoupling may, to some extent, reflect the long-term visual impairment in patients. In addition, higher cross-frequency coupling in the right posterior parietal cortex was also associated with lower severity of motor symptoms in Parkinson's disease [48]. This decoupling allows these regions to be released from the normal constraints of sensory and motor processing, which may be a potential explanation for the observed deficits. Preliminary subtype analysis did not show any significant SC-FC coupling alteration between PD subgroups. The reason might be the synchronization of SC and FC, which is heavily dictated by disease effect. In addition, considering that the sample size of each subgroup is relatively small, the test efficiency of comparison between subgroups may decrease, resulting in no significant results being found. Therefore, more robust independent studies are still warranted to confirm the hypothesis that SC-FC coupling is implicated in heterogeneity for patients with PD.

In addition to providing supporting evidence for the whole-brain SC-FC decoupling in patients with PD, a novel perspective on the network SC-FC coupling alterations of PD was offered in this study. Specifically, decreased SC-FC coupling was found in the VIS, LIM, DOR, and FPC networks and DMN. All these cortical networks are known to play a critical role in the pathogenesis of PD. Parkinson's antagonistic motor signature was dominated by networks such as VIS, SOM, FPC, and DMN, suggesting that the motor dysfunction of PD is represented as antagonistic interactions within multilevel brain system [49]. Growing evidence showed a strong involvement of the VIS system in the onset of VIS symptoms, including retinal layer thinning [50] and alterations in gray and white matter [51]. Patients with PD with poor visual function showed decreased FC [52] and increased white-matter damage over time [53]. Connectivity changes and dysfunctional integration in the LIM network have also been reported in patients with PD, and the olfactory dysfunction in PD may be associated with structural and pathological abnormalities in the LIM/paralimbic cortices [54]. The DOR module is responsible for the endogenous attention-orienting process [55], and functional impairment in the DOR network seems to be the hallmark of mild cognitive impairment due to PD, thus extending the previous findings on brain connectivity disruption in non-motor networks [56]. In addition, one study revealed that baseline akinetic/rigid symptoms are related to volumetric changes and altered FC within a

FPC network in PD [57]. According to previous research, the SC-FC in DMN was less closely aligned [40] and may be more vulnerable to the presence of neurodegeneration. Consistent with previous study [58], our separate FC analysis showed increased FC strength in DMN. Preserved SC and disrupted FC in DMN suggested that the inconsistent changes between the SC and FC networks may contribute to the SC-FC decoupling within DMN. It is possible that although no significant SC and FC changes was observed in other network, the inconsistent changes in SC and FC can be captured by SC-FC coupling.

Internetwork SC-FC coupling was also explored in this study. Altered coupling strength between SUB and cortical networks, including VIS and SOM networks, was found in PD. Structural and functional dysregulations in neural cortico-subcortical-networks could be generally observed in PD. Cognitive impairment in PD does not merely involve neurotransmitter deficits, which is also characterized by altered networks of brain structures as aggregation of degenerated α-synuclein spreads from SUB to cortical regions [59, 60]. Moreover, reduced functional connection of the VIS network to the SUB areas is related to VIS deficits frequently reported in PD [61]. The results of the present study are also largely consistent with those of previous studies that observed reduced activation and metabolism of the Parkinsonian VIS pathway in fMRI [62], PET [63], and SPECT studies [64]. In addition to VIS network, the SOM network is tightly connected to the SUB network. In the current study, increased SC-FC coupling was found between SUB and SOM networks. The SUB network and SOM formed the so-called corticobasal ganglia-thalamocortical loop, which is a fundamental circuit for motor ability and is critically related to PD [65]. Compared with HCs, SC and FC linking the SUB regions to SOM was, on average, significantly impaired in patients with PD [66]. Moreover, a study on PD showed increased internetwork variability in subnetwork pairs, including SUB network and SOM, which was significantly correlated with UPDRS-III [67]. Such alterations may ameliorate the impairment and disability in PD by enhancing the consistency between the FC and SC networks. Hence, the finding of the present study suggested that the increased SC-FC coupling between the two modules may be a compensatory mechanism to improve the performance levels in PD. In addition, the internetwork analysis confirmed that patients with PD had abnormal connections between the SOM and other networks, including DOR [68] and VEN [69]. White-matter hyper-intensity disruptions to SOM and VEN have been associated with increased postural sway when standing on an uneven surface and increased fall risk in older adults [69]. Decoupling between SOM and these subnetworks may suggest that motor dysfunctions (assessed by UPDRS-III) are associated with lower synchronization of SOM in PD [66]. Higher-order cognitive networks, including DOR, VEN, and FPC, are considered to play an important role in cognitive processing in PD [70]. In line with a data-driven result, seed-based analyses mainly revealed reduced DOR-FPC and DOR-VEN interactions and loss of normal DOR-DMN anti-correlation in patients with PD [71]. The activity in DOR and FPC is high when attention is directed externally, associated with the reduction in the activity within DMN. These networks showed anti-correlated activity, suggesting that DMN has widespread connections to the DOR and FPC, which has been suggested to be important for efficient cognitive function [72]. In addition, the negative correlation between the SC-FC coupling strengths between DOR and DMN and the UPDRS III scores indicated that SC-FC decoupling may contribute to motor impairments in PD patients. Moreover, we found that depressed PD patients had abnormal FC between insula and PCC/precuneus, and between hippocampus+amygdala and PCC [73], which indicated that the interaction between the limbic system and DMN was closely associated with depression in PD patients. However, little study has shown structural impairment between each of the above pairs of networks, which may suggest preserved SC in patients with PD. As aforementioned, the complex intranetwork and internetwork structural and functional disconnection or deactivated connectivity may account for the aberrant module-level SC-FC coupling.

Several limitations of this study should be noted. First, given the difficulty of head motion control in late-stage patients during MRI data acquisition, the sample size of patients with PD is relatively small in our study, especially in the subgroups. In the future, more multimodal brain imaging data will be combined to further explore heterogeneity and the brain network mechanism of PD. Second, this study was also based on patients with non-first-episode PD. Thus, the findings may have been potentially influenced by long-term treatment with dopaminergic medications, which should be investigated further. Third, there has not been enough effort in collecting a sufficient number of clinical scales to measure clinical symptoms, and there is still a large room for improvement. Finally, SC-FC coupling was calculated using static functional connectivity. However, some studies suggested that SC-FC coupling was altered in the dynamic acute rising phase of FC, and dynamic SC-FC coupling may reflect the flexibility by which SC relates to FC [74]. Hence, further studies concerning dynamic SC-FC coupling over time are needed in PD.

Conclusion

In summary, this work revealed the aberrant SC-FC relationship at a multiscale level in PD. In particular, SC-FC coupling was damaged at the whole-brain level, and significantly decreased SC-FC coupling was found within the VIS, DOR, LIM, and FPC modules and DMN. Decreased coupling strength between several modules mainly linking VIS, SOM, DOR, and DMN was also found in PD, and increased SC-FC coupling was found between SUB and SOM network. Although these networks may not be directly related to the onset of PD, their SC-FC coupling may be one of the potential pathogeneses of PD. Overall, these findings may provide valuable insights for further understanding of the pathophysiological network mechanisms of PD.

Supplementary Information

The online version contains supplementary material available at https://doi.org/10.1186/s12868-024-00918-4.

Supplementary Material 1

Acknowledgements
We highly appreciate all colleagues for helpful comments on the manuscript and all the selfless volunteers who participated in the study.

Author contributions
T. Z. analyzed the data, wrote and revised the main manuscript text and prepared figures; C.C.hen provided the data and wrote the main manuscript text ; H.C. designed the study and guided the methods; X.W. analyzed the data and prepared figures; L.G. analyzed the data; C.W. analyzed the data; Q.G. guided the methods; C.Z. collected the clinical data; W. L. revised the manuscript ; J.C. collected the data and interpreted the results; R.L. designed the study and guided the methods and interpreted the results.

Funding
This work was supported by the National Key R&D Program of China (2022YFC2009906), the National Natural Science Foundation of China (Nos. 62333003, 82372085, 62036003, 62173070), and the Sichuan Science and Technology Foundation (No. 2023NSFSC0644).

Data availability
The data that support the findings of this study are available from the corresponding author upon reasonable request.

Declarations

Ethics approval and consent to participate
Our study was reviewed and approved by the institutional ethics committee of the First Affiliated Hospital of Zhengzhou University. All subjects provided written informed consent before the experiment.

Consent for publication
Not applicable.

Competing interests
The authors declare no competing interests.

Received: 9 September 2024 / Accepted: 11 December 2024
Published online: 26 December 2024

References

1. Jankovic. Parkinson's disease: clinical features and diagnosis. J Neurol Neurosurg Psychiatry. 2008;79(4):368–76.
2. Weerkamp NJ, Nijhof A, Tissingh G. Non-motor symptoms of Parkinson's disease. Lancet Neurol. 2012;156(8):A3926.
3. Seppi K, Weintraub D, Coelho M, Perez-Lloret S, Fox SH, Katzenschlager R, Hametner EM, Poewe W, Rascol O, Goetz CG. The Movement Disorder Society Evidence-Based Medicine Review Update: Treatments for the non-motor symptoms of Parkinson's disease. Mov disorders: official J Mov Disorder Soc. 2011;26(S3):S2–41.
4. González-Usigli HA, Ortiz GG, Charles-Niño C, Mireles-Ramírez MA, Pacheco-Moisés FP. Torres-Mendoza BMdG, Hernández-Cruz JdJ, Delgado-Lara DLdC, Ramírez-Jirano LJ: Neurocognitive psychiatric and neuropsychological alterations in Parkinson's disease: a basic and clinical approach. Brain Sci. 2023;13(3):508.
5. Jellinger KA. Morphological basis of Parkinson disease-associated cognitive impairment: an update. J Neural Transm. 2022;129(8):977–99.
6. Tedeschi G, Russo, Antonio, Caiazzo, Giuseppina, Esposito, Fabrizio MD, Rosa. Functional connectivity underpinnings of fatigue in Drug-Naive patients with Parkinson's disease. Mov Disord 2016.
7. Koirala N, Anwar AR, Ciolac D, Glaser M, Pintea B, Deuschl G, Muthuraman M, Groppa S. Alterations in White Matter Network and Microstructural Integrity Differentiate Parkinson's Disease Patients and Healthy Subjects. Front Aging Neurosci. 2019;11:191.
8. Deng X, Liu Z, Kang Q, Lu L, Zhu Y, Xu R. Cortical Structural Connectivity Alterations and Potential Pathogenesis in Mid-Stage Sporadic Parkinson's Disease. Front Aging Neurosci. 2021;13:650371.
9. Greicius MD, Supekar K, Menon V, Dougherty RF. Resting-state functional connectivity reflects structural connectivity in the default mode network. Cereb Cortex. 2009;19(1):72–8.
10. Mishra VR, Sreenivasan KR, Yang Z, Zhuang X, Cordes D, Mari Z, Litvan I, Fernandez HH, Eidelberg D, Ritter A, et al. Unique white matter structural connectivity in early-stage drug-naive Parkinson disease. Neurology. 2020;94(8):e774–84.
11. Li R, Zou T, Wang X, Wang H, Hu X, Xie F, Meng L, Chen H. Basal ganglia atrophy–associated causal structural network degeneration in Parkinson's disease. Hum Brain Mapp. 2022;43(3):1145–56.
12. Luo CY, Song W, Chen Q, Zheng ZZ, Chen K, Cao B, Yang J, Li JP, Huang XQ, Gong QY. Reduced functional connectivity in early-stage drug-naive Parkinson's disease: a resting-state fMRI study. Neurobiol Aging. 2014;35(2):431–41.
13. Chen B, Guo GF, Hu L, Wang S. Changes in anatomical and functional connectivity of Parkinson's disease patients according to cognitive status. Eur J Radiol. 2015;84(7):1318–24.
14. Dubbelink KO, Schoonheim MM, Deijen JB, Twisk J, Barkhof F, Berendse HW. Functional connectivity and cognitive decline over 3 years in Parkinson disease. Neurology. 2014;83(22):2046.
15. Meng L, Wang H, Zou T, Wang X, Chen H, Xie F, Li R. Attenuated brain white matter functional network interactions in Parkinson's disease. Hum Brain Mapp 2022.
16. Rubinov M, Sporns O. Complex network measures of brain connectivity: uses and interpretations. NeuroImage. 2010;52(3):1059–69.
17. Suárez LE, Markello RD, Betzel RF, Misic B. Linking Structure and Function in Macroscale Brain Networks. Trends Cogn Sci. 2020;24(4):302–15.
18. Honey C, Sporns O, Cammoun L, Gigandet X. JP thiran, R. Meuli, and P. Hagman. Proc Natl Acad Sci USA. 2009;106:2035.
19. Hagmann P, Sporns O, Madan ., Cammoun N,. L, Pienaar R, Wedeen ., Meuli VJ,. R, Grant J-PT. White matter maturation reshapes structural connectivity in the late developing human brain. Proc Natl Acad Sci USA. 2018;107(44):19067–72.
20. Guerra-Carrillo B, Mackey AP, Bunge SA. Resting-state fMRI: a window into human brain plasticity. Neuroscientist. 2014;20(5):522–33.
21. Zhang Z, Liao W, Chen H, Mantini D, Ding JR, Qiang X, Wang Z, Yuan C, Chen G, Jiao Q. Altered functional-structural coupling of large-scale brain networks in idiopathic generalized epilepsy. Brain J Neurol. 2011;134(10):2912–28.
22. Baum GL, Cui Z, Roalf DR, Ciric R, Betzel RF, Larsen B, Cieslak M, Cook PA, Xia CH, Moore TM. Development of structure–function coupling in human brain networks during youth. *Proceedings of the National Academy of Sciences* 2020, 117(1):771–778.
23. Zarkali A, McColgan P, Leyland L-A, Lees AJ, Rees G, Weil RS. Organisational and neuromodulatory underpinnings of structural-functional connectivity decoupling in patients with Parkinson's disease. Commun biology. 2021;4(1):1–13.

24. Chung SJ, Shin JH, Cho KH, Lee Y, Sohn YH, Seong JK, Lee PH. Subcortical shape analysis of progressive mild cognitive impairment in Parkinson's disease. Mov Disord. 2017;32(10):1447–56.
25. Geevarghese R, Lumsden DE, Hulse N, Samuel M, Ashkan K. Subcortical structure volumes and correlation to clinical variables in Parkinson's disease. J Neuroimaging. 2015;25(2):275–80.
26. Ji JL, Spronk M, Kulkarni K, Repov G, Cole MW. Mapping the human brain's cortical-subcortical functional network organization. *NeuroImage* 2018, 185.
27. Hughes AJ, Daniel SE, Lees AJ. Improved accuracy of clinical diagnosis of Lewy body Parkinson's disease. Neurology. 2001;57(8):1497–9.
28. Goetz CG, Tilley BC, Shaftman SR, Stebbins GT, Fahn S, Martinez-Martin P, Poewe W, Sampaio C, Stern MB, Dodel R. Movement Disorder Society-sponsored revision of the Unified Parkinson's Disease Rating Scale (MDS-UPDRS): scale presentation and clinimetric testing results. Mov disorders: official J Mov Disorder Soc. 2008;23(15):2129–70.
29. HOEHN MM. Pakinsonism: onset, progression, and mortality. Neurology 1967, 17.
30. Hu Y, Li Q, Qiao K, Zhang X, Chen B, Yang Z. PhiPipe: a multi-modal MRI data processing pipeline with test–retest reliability and predicative validity assessments. Hum Brain Mapp. 2023;44(5):2062–84.
31. Modabbernia M, Whalley HC, Glahn D, Thompson PM, Kahn RS, Frangou S. Systematic Evaluation of Machine Learning Algorithms for Neuroanatomically-Based Age Prediction in Youth. Cold Spring Harbor Laboratory; 2021.
32. Schaefer A, Kong R, Gordon EM, Laumann TO, Zuo X-N, Holmes AJ, Eickhoff SB, Yeo BTT. Local-Global Parcellation of the Human Cerebral Cortex from Intrinsic Functional Connectivity MRI. Cereb Cortex. 2017;28(9):3095–114.
33. Yeo BT, Krienen FM, Sepulcre J, Sabuncu MR, Lashkari D, Hollinshead M, Roffman JL, Smoller JW, Zöllei L, Polimeni JR. The organization of the human cerebral cortex estimated by intrinsic functional connectivity. J Neurophysiol 2011.
34. Zhu D, Zhang T, Jiang X, Hu X, Chen H, Yang N, Lv J, Han J, Guo L, Liu T. Fusing DTI and fMRI data: a survey of methods and applications. NeuroImage. 2014;102:184–91.
35. Jeurissen B, Tournier J-D, Dhollander T, Connelly A, Sijbers J. Multi-tissue constrained spherical deconvolution for improved analysis of multi-shell diffusion MRI data. NeuroImage. 2014;103:411–26.
36. Tournier J-D, Connelly FCA. Improved probabilistic streamlines tractography by 2nd order integration over fibre orientation distributions. Int Soc Magn Reson Med 2010.
37. Smith RE, Tournier J-D, Calamante F, Connelly A. Anatomically-constrained tractography: Improved diffusion MRI streamlines tractography through effective use of anatomical information. NeuroImage. 2012;62(3):1924–38.
38. Smith RE, Tournier J-D, Calamante F, Connelly A. SIFT2: Enabling dense quantitative assessment of brain white matter connectivity using streamlines tractography. NeuroImage. 2015;119:338–51.
39. Ashburner J. A fast diffeomorphic image registration algorithm. NeuroImage. 2007;38(1):95–113.
40. Gu Z, Jamison KW, Sabuncu MR, Kuceyeski A. Heritability and interindividual variability of regional structure-function coupling. Nat Commun. 2021;12(1):1–12.
41. Zhao S, Wang G, Yan T, Xiang J, Yu X, Li H, Wang B. Sex differences in anatomical rich-club and structural–functional coupling in the human brain network. Cereb Cortex. 2021;31(4):1987–97.
42. Wüllner U, Borghammer P, Choe C-u, Csoti I, Falkenburger B, Gasser T, Lingor P, Riederer P. The heterogeneity of Parkinson's disease. J Neural Transm. 2023;130(6):827–38.
43. Burdick DJ, Cholerton B, Watson GS, Siderowf A, Trojanowski JQ, Weintraub D, Ritz B, Rhodes SL, Rausch R, Factor SA. People with Parkinson's disease and normal MMSE score have a broad range of cognitive performance. Mov Disorders Official J Mov Disorder Soc. 2015;29(10):1258–64.
44. Tan YW, Liu L, Wang YF, Li HM, Pan MR, Zhao MJ, Huang F, Wang YF, He Y, Liao XH. Alterations of cerebral perfusion and functional brain connectivity in medication-naïve male adults with attention-deficit/hyperactivity disorder. CNS Neurosci Ther. 2020;26(2):197–206.
45. Emerson RW. Parametric tests, their nonparametric alternatives, and degrees of freedom. J Visual Impairment Blindness. 2016;110(5):377–80.
46. Jia G, Peng X, Chao S, Li Y, Zhao X. Characterizing structure connectivity correlation with the default mode network in Alzheimer's patients and normal controls. Proc SPIE-Int Soc Opt Eng. 2012;8317:61.
47. Tomasino B, Gremese M. Effects of Stimulus Type and Strategy on Mental Rotation Network: An Activation Likelihood Estimation Meta-Analysis. Front Hum Neurosci. 2015;9:693.
48. Bin Yoo H, De Concha EOdl D, Pickut BA, Vanneste S. The functional alterations in top-down attention streams of Parkinson's disease measured by EEG. Sci Rep. 2018;8(1):10609.
49. Wang X, Yoo K, Chen H, Zou T, Wang H, Gao Q, Meng L, Hu X, Li R. Antagonistic network signature of motor function in Parkinson's disease revealed by connectome-based predictive modeling. NPJ Parkinson's disease. 2022;8(1):1–13.
50. Lee JY, Kim JM, Ahn J, Kim HJ, Jeon BS, Kim TW. Retinal nerve fiber layer thickness and visual hallucinations in Parkinson's disease. Mov Disord. 2014;29(1):61–7.
51. Arrigo A, Calamuneri A, Aragona E, Mormina E, Gaeta M. Visual impairment in Parkinson's disease. 2020.
52. Hepp DH, Foncke EM, Olde Dubbelink KT, van de Berg WD, Berendse HW, Schoonheim MM. Loss of functional connectivity in patients with Parkinson disease and visual hallucinations. Radiology. 2017;285(3):896–903.
53. Zarkali A, McColgan P, Leyland LA, Lees AJ, Weil RS. Visual dysfunction predicts cognitive impairment and white matter degeneration in Parkinson's disease. Mov Disord. 2021;36(5):1191–202.
54. Su M, Wang S, Fang W, Zhu Y, Li R, Sheng K, Zou D, Han Y, Wang X, Cheng O. Alterations in the limbic/paralimbic cortices of Parkinson's disease patients with hyposmia under resting-state functional MRI by regional homogeneity and functional connectivity analysis. Parkinsonism Relat Disord. 2015;21(7):698–703.
55. Fox M, Corbetta M, Snyder AZ, Vincent JL, Raichle ME, Fox MD, Corbetta M, Snyder AZ, Vincent JL, Raichle ME. Spontaneous neuronal activity distinguishes human dorsal and ventral attention systems. Proc Natl Acad Sci USA 103: 10046–10051. *Proceedings of the National Academy of Sciences* 2006, 103(26):10046–10051.
56. Bezdicek O, Ballarini T, Růžička F, Roth J, Mueller K, Jech R, Schroeter ML. Mild cognitive impairment disrupts attention network connectivity in Parkinson's disease: a combined multimodal MRI and meta-analytical study. Neuropsychologia. 2018;112:105–15.
57. Kann SJ, Chang C, Manza P, Leung HC. Akinetic rigid symptoms are associated with decline in a cortical motor network in Parkinson's disease. NPJ Parkinson's disease. 2020;6:19.
58. Hou Y, Luo C, Yang J, Ou R, Liu W, Song W, Gong Q, Shang H. Default-mode network connectivity in cognitively unimpaired drug-naïve patients with rigidity-dominant Parkinson's disease. J Neurol. 2017;264(1):152–60.
59. Pandya S, Zeighami Y, Freeze B, Dadar M, Collins DL, Dagher A, Raj A. Predictive model of spread of Parkinson's pathology using network diffusion. NeuroImage. 2019;192:178–94.
60. Yau Y, Zeighami Y, Baker T, Larcher K, Vainik U, Dadar M, Fonov V, Hagmann P, Griffa A, Mišić B. Network connectivity determines cortical thinning in early Parkinson's disease progression. Nat Commun. 2018;9(1):1–10.
61. Bodis-Wollner I, Tagliati M. The visual system in Parkinson's disease. Adv Neurol. 1993;60:390–4.
62. Meppelink AM, de Jong BM, Renken R, Leenders KL, Cornelissen FW, van Laar T. Impaired visual processing preceding image recognition in Parkinson's disease patients with visual hallucinations. Brain. 2009;132(11):2980–93.
63. Park HK, Kim JS, Im KC, Kim MJ, Lee JH, Lee MC, Kim J, Chung SJ. Visual Hallucinations and Cognitive Impairment in Parkinson's Disease. Can J Neurol Sci. 2013;40(05):657–62.
64. Matsui H, Nishinaka K, Oda M, Hara N, Komatsu K, Kubori T, Udaka F. Hypoperfusion of the visual pathway in parkinsonian patients with visual hallucinations. Mov disorders: official J Mov Disorder Soc. 2006;21(12):2140–4.
65. Alexander GE, Delong M, Strick P. Parallel Organization of Functionally Segregated Circuits Linking Basal Ganglia and Cortex. Annu Rev Neurosci. 1986;9(1):81–357.
66. Liu S, Zhao Y, Ren Q, Zhang D, Shao K, Lin P, Yuan Y, Dai T, Zhang Y, Li L. Amygdala abnormalities across disease stages in patients with sporadic amyotrophic lateral sclerosis. Hum Brain Mapp. 2022;43(18):5421–31.
67. Zhu H, Huang J, Deng L, He N, Cheng L, Shu P, Yan F, Tong S, Sun J, Ling H. Abnormal Dynamic Functional Connectivity Associated With Subcortical Networks in Parkinson's Disease: A Temporal Variability Perspective. Front NeuroSci. 2019;13:80.
68. Palmer WC, Cholerton BA, Zabetian CP, Montine TJ, Rane S. Resting-State Cerebello-Cortical Dysfunction in Parkinson's Disease. Front Neurol. 2021;11:594213.
69. Crockett RA, Hsu CL, Dao E, Tam R, Alkeridy W, Eng JJ, Handy TC, Liu-Ambrose T. Mind the Gaps: Functional Networks Disrupted by White Matter Hyperintensities Are Associated with Greater Falls Risk. Neurobiol Aging. 2021;109:166–75.

70. Baggio HC, Segura B, Sala-Llonch R, Marti MJ, Valldeoriola F, Compta Y, Tolosa E, Junque C. Cognitive impairment and resting-state network connectivity in P arkinson's disease. Hum Brain Mapp. 2015;36(1):199–212.
71. Campbell MC, Jackson JJ, Koller JM, Snyder AZ, Kotzbauer PT, Perlmutter JS. Proteinopathy and longitudinal changes in functional connectivity networks in Parkinson disease. Neurology. 2020;94(7):e718–28.
72. Hou Y, Yang J, Luo C, Song W, Ou R, Liu W, Gong Q, Shang H. Dysfunction of the Default Mode Network in Drug-Naive Parkinson's Disease with Mild Cognitive Impairments: A Resting-State fMRI Study. Front Aging Neurosci. 2016;8:247.
73. Lin H, Cai X, Zhang D, Liu J, Na P, Li W. Functional connectivity markers of depression in advanced Parkinson's disease. NeuroImage: Clin. 2020;25:102130.
74. Bi K, Hua L, Wei M, Qin J, Lu Q, Yao Z. Dynamic functional–structural coupling within acute functional state change phases: evidence from a depression recognition study. J Affect Disord. 2016;191:145–55.

Publisher's note